enthalpy recovery peaks of the pure components increases as a function of aging time since the component with the lowest T_g approaches equilibrium after a short aging time.

Finally, it is important to realize that multiple enthalpy recovery peaks may also occur in pure polymer systems.[31] Therefore, conclusions concerning phase behavior of polymer blends based on the enthalpy recovery method always require a comparison between the enthalpy recovery behavior of the blend and of the pure components.

Acknowledgment. It is a pleasure to acknowledge Y. Y. Tan for his suggestion to apply the enthalpy recovery method to the P2VP/PS system.

Registry No. PS, 9003-53-6; P2VP, 25014-15-7.

References and Notes

(1) Bosma, M.; ten Brinke, G.; Ellis, T. S. *Macromolecules* **1988**, *21*, 1465.
(2) Kambour, R. P.; Bendler, J. T.; Bopp, R. C. *Macromolecules* **1983**, *16*, 753.
(3) Ten Brinke, G.; Karasz, F. E.; MacKnight, W. J. *Macromolecules* **1983**, *16*, 1827.
(4) Paul, D. R.; Barlow, J. W. *Polymer* **1984**, *25*, 487.
(5) Woo, E. M.; Barlow, J. W.; Paul, D. R. *Polymer* **1985**, *26*, 763.
(6) Barlow, J. W.; Paul, D. R. *Polym. Eng. Sci.* **1987**, *27*, 1482.
(7) Olabishi, O.; Robeson, L. M.; Shaw, M. T. *Polymer–Polymer Miscibility*; Academic Press: New York, 1979.
(8) Hodge, I. M.; Berens, A. R. *Macromolecules* **1982**, *15*, 762.
(9) DeBolt, M. A.; Easteal, A. J.; Macedo, P. B.; Moynihan, C. T. *J. Am. Ceram. Soc.* **1976**, *59*, 16.
(10) Moynihan, C. T.; et. al. *Ann. N. Y. Acad Sci.* **1976**, *279*, 15.
(11) Kovacs, A. J.; Aklonis, J. J.; Hutchinson, J. M.; Ramos, A. R. *J. Polym. Sci., Polym. Phys. Ed.* **1979**, *17*, 1079.
(12) Nagi, K. L. *Comments Solid State Phys.* **1979**, *9*, 127; **1980**, *9*, 141.
(13) Robertson, R. E.; Simha, R.; Curro, J. G. *Macromolecules* **1984**, *17*, 911.
(14) *Relaxations in Complex Systems*; Ngai, K. L., Wright, G. B., Eds.; U.S. Government Printing Office: Washington, DC, 1985. (Available from National Technical Information Service, 5285 Port Royal Road, Springfield, VA 22161.)
(15) McKenna, G. B. In *Comprehensive Polymer Science*; Booth, C., Price, C., Eds.; Pergamon Press: Oxford, 1988; Vol. 2, Properties.
(16) Rendell, R. W.; Ngai, K. L.; Fong, G. R.; Aklonis, J. J. *Macromolecules* **1987**, *20*, 1070.
(17) Tool, A. Q. *J. Am. Ceram. Soc.* **1946**, *29*, 240.
(18) Gardon, R.; Narayanaswamy *J. Am. Ceram. Soc.* **1970**, *53*, 148.
(19) Narayanaswamy *J. Am. Ceram. Soc.* **1971**, *54*, 491.
(20) Hodge, I. M. In ref 14, p 65.
(21) Margaritis, A. G.; Kallitsis, J. K.; Kalfoglou, N. K. *Polymer* **1987**, *22*, 2122.
(22) Cowie, J. M. G.; Lath, D. *Makromol. Chem., Macromol. Symp.* **1988**, *16*, 103.
(23) Illers, K. H. *Makromol. Chem.* **1969**, *127*, 1.
(24) Gray, A.; Gilbert, M. *Polymer* **1976**, *17*, 44.
(25) Berens, A. R.; Hodge, I. M. *Macromolecules* **1982**, *15*, 756.
(26) Kovacs, A. J. *Fortschr. Hochpolym. Forsch.* **1963**, *3*, 394.
(27) Shaw, M. T. *J. Appl. Polym. Sci.* **1974**, *18*, 449.
(28) Hodge, I. M.; Huvard, G. S. *Macromolecules* **1983**, *16*, 371.
(29) Privalko, V. P.; Demchenko, S. S.; Lipatov, Y. S. *Macromolecules* **1986**, *19*, 901.
(30) Hodge, I. M.; Berens, A. R. *Macromolecules* **1981**, *14*, 1599.
(31) Ruddy, M.; Hutchinson, J. M. *Polym. Commun.* **1988**, *29*, 132.
(32) Ellis, T. S.; Karasz, F. E. *Polym. Eng. Sci.* **1986**, *26*, 290.
(33) Matsushita, Y.; Nakao, Y.; Saguchi, R.; Choshi, H.; Nagasawa, M. *Polym. J. (Tokyo)* **1986**, *18*, 493.
(34) Hadziioannou, G., private communications.
(35) Creton, C.; Kramer, E. J.; Hadziioannou, G. *Bull. Am. Phys. Soc.* **1988**, *33*, 586.

Clearing Temperatures of Aramid Solutions in Sulfuric Acid

S. J. Picken*

Akzo Research, Corporate Research Department, Arnhem, Postbox 9300,
6800 SB ARNHEM, The Netherlands.
Received July 25, 1988;
Revised Manuscript Received September 27, 1988

ABSTRACT: Measurements of the nematic–isotropic transition temperatures of solutions of poly(*p*-phenyleneterephthalamide), poly(*p*-benzamide), and poly(4,4′-benzanilidyleneterephthalamide) in concentrated sulfuric acid are presented as a function of concentration and average molecular weight. The results indicate a strong influence of molecular flexibility on the clearing temperature. The experiments are explained by a mean-field theory analogous to the Maier–Saupe theory for low molecular weight nematic liquid crystals.

Introduction

In this paper measurements of the nematic–isotropic transition (or clearing) temperatures of solutions of PPTA (poly(*p*-phenyleneterephthalamide)) and other aramids in concentrated H_2SO_4 are presented. The results show a marked influence of polymer concentration on the clearing temperature. The slope of the concentration–clearing temperature graphs depends on the average molecular weight of the polymer. This indicates a coupling of the (temperature dependent) molecular flexibility to the phase transition.

Molecular flexibility is usually described by the so-called persistence length. An influence of temperature on the persistence length has been found experimentally for a variety of materials, e.g., (acetoxypropyl)cellulose[1] and can also be derived theoretically from a wormlike model for polymer chains (see Appendix).

Basically two mechanisms can lead to formation of a nematic phase: the first is dealt with in the traditional Onsager or Flory type of approach.[2,3] This shows that, depending on the axial ratio of the rodlike particles, there is a critical concentration above which a nematic phase is formed. This concentration does not depend on the temperature of the system as these theories are essentially athermal; i.e., the part of the free energy that leads to the anisotropy is an entropy term.

A later version of the Flory theory describes a system of semiflexible particles. The persistence length is used to determine an effective axial ratio for the particles.[4] A temperature-dependent persistence length thus leads to a "thermotropic" type of behavior where the phase transition is governed by the temperature as well as the concentration.

An alternative mechanism is used by the Maier-Saupe mean field theory.[5] Here the stability of the nematic phase is explained from an anisotropic potential. Despite the complete neglect of the excluded-volume (entropy) terms in the free energy, the temperature dependence of the $\langle P_2 \rangle$

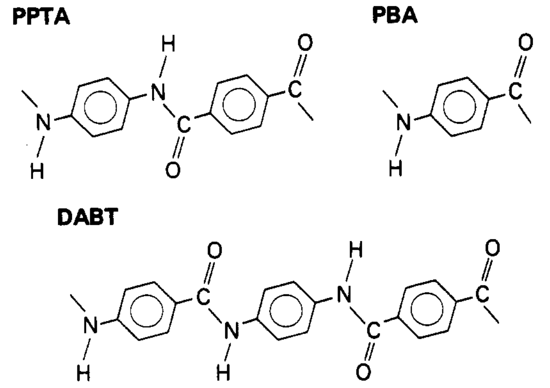

Figure 1. Aramids that were studied.

Table I[a]

sample	$\bar{M}_w$	A	α
PPTA	12000	46 (4)	0.85 (0.04)
PPTA	31000	99 (2)	0.56 (0.01)
DABT	8000	37 (2)	0.92 (0.03)
DABT	42000	74 (5)	0.66 (0.03)
DABT	70000	115 (10)	0.49 (0.04)
PBA	10000	41 (6)	0.92 (0.06)

[a] A and α are from least-squares fits of the clearing temperature (T_{ni}) versus concentration (c) measurements to a relation of the form $T_{ni} = Ac^{\alpha}$. The standard deviations of A and α are shown in parentheses.

order parameter of many low molecular weight system is predicted rather well by this approach.[6]

The experiments described here are explained by a modified Maier–Saupe mean-field theory. The influence of concentration and molecular flexibility is taken into account via the strength of the anisotropic potential. This is done by using simple power-law relations.

Experimental Section

Measurements of the nematic–isotropic transition temperatures were performed on solutions of PPTA (poly(*p*-phenyleneterephthalamide)), DABT (poly(4,4′-benzanalidyleneterephthalamide)), and PBA (poly(*p*-benzamide) (see Figure 1) in concentrated (99.8%) H_2SO_4. The anisotropic solutions were prepared by dissolving the polymers in H_2SO_4 (99.8%). In each case about 2 g of solution was made. The molecular weight ($\bar{M}_w$) of the samples was estimated from viscosity measurements. The calibration curve we used was obtained from GPC, HP-SEC, light-scattering, and end-group analysis methods. The polymer samples are listed in Table I.

The clearing temperatures (T_{ni}) were determined at various concentrations by polarization microscopy. We used a Leitz Orthoplan-Pol polarizing microscope with a Mettler FP800/82 hot stage. The value of T_{ni} was determined by measuring 10 samples at a heating rate of 5 °C/min, where T_{ni} is the temperature at which 50% phase separation is observed. Taking the average of these measurements leads to a reasonably accurate and reproducible value for T_{ni} (within approximately 1 °C or less).

Possible degradation of the polymer was investigated by cooling the sample and performing a second measurement. This is mainly of interest for the higher concentrations. For the measurements shown, no difference was found for the first and second measurements. If the temperature is higher than approximately 130 °C, the degradation of the sample prevents accurate determination of T_{ni}.

In principle the presence of water can also lead to serious problems for the reproduction of the results. We found that preheating the sample slides to about 50 °C before applying the polymer solution leads to homogeneous samples and reproducible results. If this procedure is not used we find "isotropic" regions in the samples. This effect is possibly caused by a thin boundary layer of water on the glass slides that is removed by the preheating treatment.

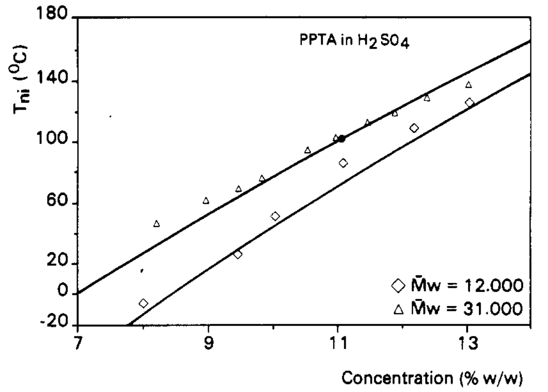

Figure 2. Clearing temperature T_{ni} as a function of polymer concentration (w/w) PPTA in 99.8% H_2SO_4. The average molecular weights $\bar{M}_w$ are indicated by the different symbols. The drawn curves are from the theory described in the text.

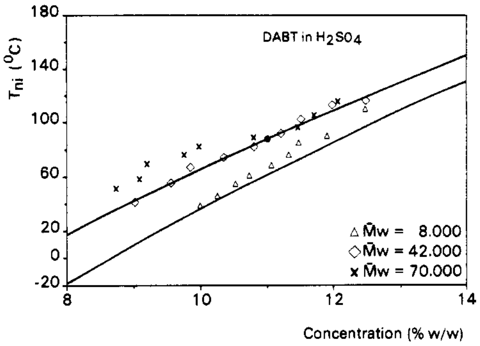

Figure 3. Figure 2 but for DABT.

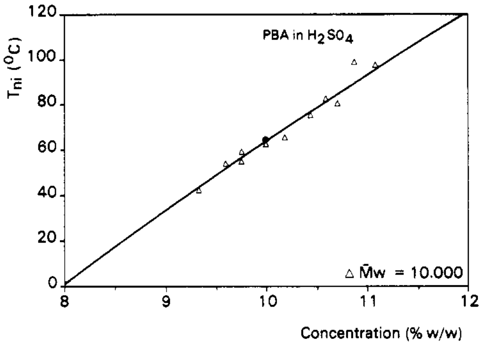

Figure 4. Figure 2 but for PBA.

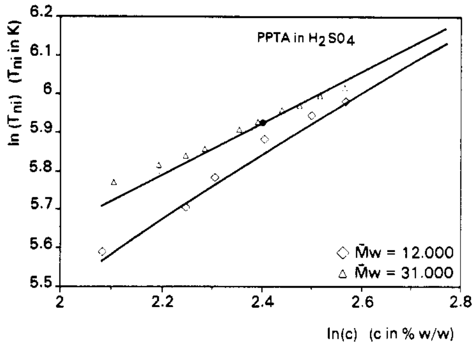

Figure 5. Natural logarithm of T_{ni} (kelvin) versus the natural logarithm of the PPTA concentration (w/w) in H_2SO_4 (99.8%). The values for $\bar{M}_w$ are indicated by the symbols. The drawn curves are from the theory described in the text.

The results are shown in Figures 2–4 and are also given in Figures 5–7, using logarithmic temperature and concentration scales, where T_{ni} is in kelvin and c in percent (w/w). The values of A and α from a least-squares fit of the data to a relation of the form $T_{ni} = Ac^{\alpha}$ are shown in Table I. The curves shown in

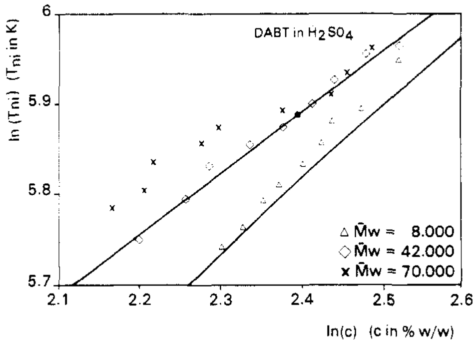

Figure 6. Figure 5 but for DABT.

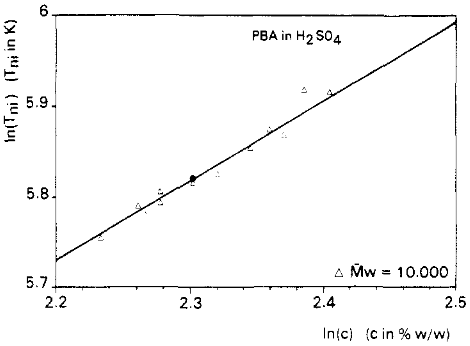

Figure 7. Figure 5 but for PBA.

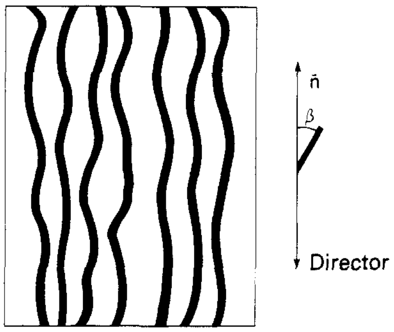

Figure 8. Nematic phase of wormlike polymer molecules, indicated by the thick lines. The angle β with respect to the local director is shown.

the figures are obtained from a mean-field theory that is described in the following and should not be confused with the least-squares fits.

A few general observations can be made from the measurements: first, we observe that higher molecular weights lead to somewhat higher values for T_{ni} although this effect is not dramatic. Second, the low molecular weight samples show a much stronger influence of the concentration on T_{ni} than the high molecular weight samples.

The Modified Maier–Saupe Mean-Field Theory

The chance to find a molecule at an angle β with respect to the director or average orientation axis is given by (see Figure 8)

$$N(\beta)\,\mathrm{d}\beta \equiv f(\beta)\sin(\beta)\,\mathrm{d}\beta \tag{1}$$

The function $f(\beta)$ is called the orientational distribution function.

In general the orientational distribution function depends on all three Eulerian angles. The use of eq 1 implicitly means that we are excluding the possibility of biaxial phases and the influence of molecular flatness. This is due to the fact that the angle β is only related to the degree of long axis orientation of the molecules. In most cases, however, the description of the nematic phase using eq 1 is quite good.

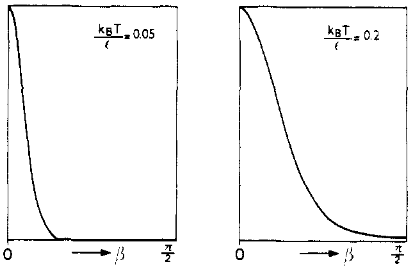

Figure 9. Orientational distribution function $f(\beta)$ from the Maier–Saupe theory for $k_BT/\epsilon = 0.05$ and 0.2. The vertical axes are scaled to the maximum value $f(0)$.

The standard Maier–Saupe theory is based on an effective potential that leads to macroscopic orientational order[5,10]

$$U = -\epsilon\langle P_2\rangle P_2(\cos(\beta)) \tag{2}$$

where ϵ is an arbitrary positive constant determining the strength of the orienting potential and $\langle P_2\rangle$ is the average value of $P_2(\cos(\beta)) = {}^1/_2(3\cos^2(\beta) - 1)$, the second-order Legendre polymomial. $\langle P_2\rangle$ is usually called the order parameter.

The value of $\langle P_2\rangle$ describes the degree of order present: if $\langle P_2\rangle = 1$ one has perfect alignment of the molecules and if $\langle P_2\rangle = 0$ there is no macroscopic orientational order (i.e., the isotropic phase). The orienting potential U satisfies the symmetry requirements of the nematic phase (i.e., uniaxial up–down symmetry) and due to the presence of $\langle P_2\rangle$ disappears in the isotropic phase, as expected.

Using this potential one obtains

$$f(\beta) = \frac{1}{\zeta}\exp\left(\frac{\epsilon}{k_BT}\langle P_2\rangle P_2(\cos\beta)\right) \tag{3}$$

with ζ the partition function

$$\zeta = \int_{-1}^{1}\mathrm{d}(\cos\beta)\exp\left(\frac{\epsilon}{k_BT}\langle P_2\rangle P_2(\cos\beta)\right) \tag{4}$$

$\langle P_2\rangle$ is found from

$$\langle P_2\rangle = \frac{1}{\zeta}\int_{-1}^{1}\mathrm{d}(\cos\beta)\,P_2(\cos\beta)\exp\left(\frac{\epsilon}{k_BT}\langle P_2\rangle P_2(\cos\beta)\right) \tag{5}$$

Note that $\langle P_2\rangle = 0$ is a solution of eq 5. Additional solutions for $\langle P_2\rangle$ are found for low values of k_BT/ϵ. The solution with the lowest value for the free energy is the stable one. This is found to correspond to the nematic phase. Thus given k_BT/ϵ, one can solve $\langle P_2\rangle$ from eq 5 and find $f(\beta)$ from eq 3 and 4. This leads to an approximately Gaussian distribution of the molecules along the macroscopic axis that broadens with increasing temperature k_BT/ϵ (see Figure 9). A first order phase transition, from the nematic to the isotropic phase, occurs at $k_BT/\epsilon \simeq 0.22$. The critical value of $\langle P_2\rangle$ at the phase transition is about 0.43. The temperature dependence of $\langle P_2\rangle$ is shown in fig. 10. Observe that the clearing temperature is directly proportional to ϵ.

This standard Maier–Saupe mean-field theory has to be modified before application to lyotropic polymer liquid crystals. First, the influence of the concentration of the polymer molecules has to be taken into account. And second, the polymer molecules are (semi-) flexible. Molecular flexibility is often described by the persistence length, L_p, which can be determined by light-scattering methods. The persistence length for PPTA in dilute (i.e., isotropic) solutions is found to be 29 ± 5 nm,[7] whereas the contour length for a characteristic molecular weight of say

30 000 amu is 170 nm. This is calculated by using a monomer mass of 238 amu and a monomer length of 1.29 nm. From this we conclude that aramid molecules although stiff are far from being rigid.

To extend the Maier–Saupe theory to lyotropic PLC systems, we return to the expression for the orienting potential (eq 2). The parameter ϵ will now be adapted to take concentration and molecular flexibility into account.

Regarding the influence of concentration we choose ϵ to be proportional to c^γ. According to an analysis by Cotter[8] the exponent γ is expected to be 1. However, the influence of pressure on the clearing temperature of low molecular weight nematics indicates that higher values (as high as 4) are found experimentally for this exponent. This is discussed in more detail by Luckhurst in ref 9. Here we are assuming that the density for a low molecular weight system is analogous to the concentration in the present case.

As regards the influence of flexibility, first some remarks will be made on the persistence length. For an infinite semiflexible chain, one can derive that the persistence length is proportional to $1/T$ (see Appendix). This has been used before by several authors.[10,11] From experiments on cellulose derivatives, the temperature dependence would seem to be even stronger with exponents of −1.6 to −3.7.[12] We feel that this can possibly be explained from the breaking of the intrachain hydrogen bonds in cellulose. For this reason we will use the standard $1/T$ dependence for aramids. We now define L_p, the persistence length at temperature T_p, and L_c, the average contour length of a polymer chain. In the Appendix the following expression for the temperature dependence of the "contour projection length" $L(T)$ of a finite continuous semiflexible chain is derived:

$$L(T) = L_p \frac{1 - \exp\left(-\dfrac{L_c T}{L_p T_p}\right)}{T/T_p} \qquad (6)$$

We define the contour projection length as the projection of a polymer chain along the direction of the first "segment". The limiting value for an infinite chain is just the persistence length, whereas the value for a very short molecule is just the end-to-end distance. This means that $L(T)$ describes the rigidity of a semiflexible polymer for all molecular weights. For low molecular weights such polymers are essentially inflexible. For a high molecular weight the degree of rigidity is characterized by the persistence length rather than the contour length. In the model the molecular weight dependence of T_{ni} comes from the influence of L_c on $L(T)$. We use only $\bar{M}_w$ for our model and do not consider the effect of the molecular weight distribution.

The influence of the flexibility of the molecules on ϵ is taken into account by postulating

$$\epsilon \sim (L(T))^\delta \qquad (7)$$

The value of the exponent δ is not easily estimated. Assuming that ϵ is proportional to L, i.e., $\delta = 1$, would seem reasonable from the point of view that increasing the length of a "test rod" in a nematic environment by a certain factor would increase the orienting potential by the same amount. On the other hand one can argue that a two-particle interaction would scale as L^2. Reasonable values for δ are thus somewhere between 1 and 2. For generality we will leave δ as a parameter in the equations. When comparing the calculations with the experiments we, however, will use the value of 2, as this seems to give the best results. Combining both the influence of concentration and that of flexibility on ϵ leads to

$$\epsilon = \epsilon^* c^\gamma (L_p)^\delta \left(\frac{1 - \exp\left(-\dfrac{L_c T}{L_p T_p}\right)}{T/T_p} \right)^\delta \qquad (8)$$

To estimate the influence of concentration on the clearing point we can study two extreme cases: the infinite chain and the rigid rod. The experimental dependence is described quite well by

$$T_{ni} = Ac^\alpha \qquad (9)$$

Using this we now easily derive for the infinite chain limit

$$T_{ni} \sim c^\alpha \sim \epsilon \sim (L(T_{ni}))^\delta c^\gamma \sim T_{ni}^{-\delta} c^\gamma \sim c^{\gamma - \alpha\delta}$$

thus $c^{\gamma-\alpha\delta} \sim c^\alpha$ and $\alpha = \gamma/(\delta + 1)$. For the rigid-rod limit we of course find $\alpha = \gamma$, as the influence of flexibility can be disregarded.

We will now compare the model (eq 8) with the experimental results in Figures 2–7. The clearing temperature T_{ni} is given by $T_{ni} = 0.22\epsilon/k_B$ and ϵ is given in eq 8. We use a value of 2 for both the exponents γ and δ. This is in agreement with the observation that dispersive interactions scale as $1/r^6$ (van der Waals) or $1/V^2$ or c^2 and that the Maier–Saupe potential is an average over all two-particle interactions leading to an L^2 dependence. Other values for the exponents give less satisfactory agreement of the theory with the experiments. Of course the value of ϵ^* in eq 8 has to be determined from the measurements. The point that was used is indicated by a filled circle in each of the figures. We find that the model gives quite reasonable quantitative agreement with the experiments. Both the slope of the concentration–T_{ni} graphs and the influence of the molecular weight are described quite well. For PBA and PPTA the agreement is good. For DABT the experimental results for $\bar{M}_w = 70\,000$ are not explained by the model. The calculated values of T_{ni} for $\bar{M}_w = 42\,000$ and 70 000 are the same due to the fact that the contour length is substantially larger than the persistence length in both cases. The experimental difference is possibly caused by the very high viscosity of the $\bar{M}_w = 70\,000$ solutions, leading to a slow response of the solutions to a temperature sweep. Indeed, at higher temperatures the difference between $\bar{M}_w = 42\,000$ and 70 000 seems to be rather small.

The temperature dependence of $\langle P_2 \rangle$ from our model is shown in Figure 10 for the infinite chain limit. The parameters were chosen so as to obtain the same clearing temperature as with the standard Maier–Saupe theory, for easy comparison. The $\langle P_2 \rangle$ order parameter is more sensitive to changes in temperature with our model. This is due to the increasing rigidity of the polymer chain with decreasing temperature.

Finally we would like to note that for the clearing temperature in thermotropic polyesters with various lengths of the spacers, we have found an exponent of about 0.6 in the T_{ni} versus monomer length dependence. We take the odd–even effect into account by comparing only odd or only even numbers of the homologous series. As the monomer length varies as a function of the length of the flexible spacer, one can relate this effect to a "concentration" of rigid aromatic groups in an aliphatic "solvent" (the spacers). The value of this exponent seems to be an almost universal property of the NI transition in thermotropic polymer liquid crystals (e.g., ref 13–15) and also agrees with $\alpha = 0.66$ from our model for the high molecular weight limit using γ and $\delta = 2$. This agreement could, however, just be a matter of coincidence.

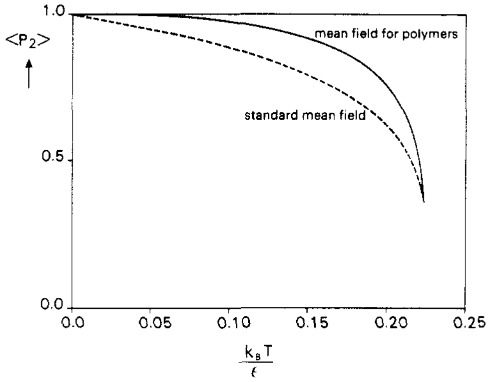

Figure 10. $\langle P_2\rangle$ order parameter as a function of k_BT/ϵ from the Maier–Saupe theory (dotted line). The drawn curve is from the model described here, for the infinite chain limit; the x-axis was scaled to the standard theory for easy comparison.

Discussion

Various objections can be raised to our model from a fundamental point of view, for instance the excluded-volume term in the free energy is completely disregarded, and the extension of the Maier–Saupe model is performed by using rather ad hoc methods. Nevertheless we feel that the ability to explain the experiments provides a certain justification of our line of approach. At any rate various essential properties of lyotropic polymer liquid crystals are taken into account.

The combination of a wormlike model and a Maier–Saupe-type model has also been suggested by Jähnig[10] and is developed further by ten Bosch, Maissa, and Sixou[16] as well as by Warner et al.[11] Their models have not yet been compared with our experimental results but would seem to be quite promising. Indeed, by using $\epsilon = \epsilon^*c$ where ϵ is the strength of the dispersion interaction per unit length, one readily finds $T_{\rm ni} \sim (\epsilon\alpha a)^{1/2} \sim c^{1/2}$ for the high w limit. This is in agreement with our experimental results. A more detailed study of these theories is planned.

A more stringent experimental test for our theory would be the determination of the temperature dependence of the order parameter in aramid solutions. Currently such measurements are under way and will be reported on in a future publication.

Despite the success in explaining the experiments, we feel that ultimately a theory, along the lines of, e.g., Khokhlov and Semenov,[17] that includes both the excluded-volume interaction and a Maier–Saupe term should be capable of explaining the experiments. As yet, however, we have not succeeded in obtaining the observed influence of concentration on the clearing temperature from their theory.

Acknowledgment. I thank Dr. J. J. van Aartsen, Dr. M. G. Northolt, Dr. S. van der Zwaag, Prof. H. N. W. Lekkerkerker, and Prof. T. Odijk for stimulating discussions and their continued interest in this work.

Appendix: Derivation of the Contour Projection Length

The polymer is modeled as a segmented chain where the rigid subsegments (of length a) are oriented parallel to each other by an orienting potential U

$$U = -\alpha \cos(\theta)$$

The orientational distribution function of a segment, assuming a fixed orientation of the previous one, is given by

$$f(\theta) = \zeta^{-1} \exp\left(\frac{\alpha}{k_bT}\cos(\theta)\right)$$

with

$$\zeta = \int_{-1}^{1} \mathrm{d}(\cos(\theta)) \exp\left(\frac{\alpha}{k_BT}\cos(\theta)\right) = \frac{2k_BT}{\alpha}\sinh\left(\frac{\alpha}{k_BT}\right)$$

Now the average deviation angle is given by

$$\langle\cos(\theta)\rangle = \frac{\langle\vec{a}_n\cdot\vec{a}_{n+1}\rangle}{a^2} = \zeta^{-1}\int_{-1}^{1}\mathrm{d}(\cos(\theta))\exp\left(\frac{\alpha}{k_BT}\cos(\theta)\right)\cos(\theta)$$

Assuming that the correlation between subsequent subsegments is large, i.e., α/k_BT is large, one finds

$$\langle\cos(\theta)\rangle = \coth\left(\frac{\alpha}{k_BT}\right) - \frac{k_BT}{\alpha} \approx 1 - \frac{k_BT}{\alpha}$$

The condition mentioned above can be satisified by choosing a sufficiently small length of a subsegment.

The persistence length is obtained from the following expression

$$L_{\rm p}(T) = a\sum_{n=0}^{\infty}\langle\cos(\theta)\rangle^n = \frac{a}{1-\langle\cos(\theta)\rangle} = \frac{\alpha a}{k_BT}$$

Thus it follows that

$$L_{\rm p}(T) \sim 1/T$$

i.e., the persistence length is proportional to the reciprocal of the temperature.

For a finite chain we similarly derive ($L_{\rm c} = Na$)

$$L(T) = a\sum_{n=0}^{N-1}\langle\cos(\theta)\rangle^n = \frac{L_{\rm c}}{N}\,\frac{1-\left(\coth\left(\frac{\alpha}{k_BT}\right)-\frac{k_BT}{\alpha}\right)^N}{1-\left(\coth\left(\frac{\alpha}{k_BT}\right)-\frac{k_BT}{\alpha}\right)}$$

Now taking the continuous limit where $N \rightarrow \infty$, $\alpha \rightarrow \infty$, and $\alpha = KN$ we find

$$L(T) = \lim_{\substack{N\to\infty \\ \alpha=KN}} \frac{L_{\rm c}}{N}\,\frac{1-\left(1-\frac{k_BT}{NK}\right)^N}{1-\left(1-\frac{k_BT}{NK}\right)} = L_{\rm c}\frac{1-\exp\left(-\frac{k_BT}{K}\right)}{k_BT/K}$$

Requiring that $L(T_{\rm p}) = L_{\rm p}$ (the persistence length at temperature $T_{\rm p}$) for an *infinite* chain length, we find for K:

$$K = \frac{L_{\rm p}}{L_{\rm c}}k_BT_{\rm p}$$

And thus

$$L(T) = L_{\rm p}\frac{1-\exp\left(-\frac{L_{\rm c}T}{L_{\rm p}T_{\rm p}}\right)}{T/T_{\rm p}}$$

Registry No. PBZ (homopolymer), 25136-77-0; PBA (SRU), 24991-08-0; PPTA (copolymer), 25035-37-4; PPTA (SRU), 24938-64-5; DABT (copolymer), 29153-47-7.

References and Notes

(1) Laivins, G. V.; Gray, D. G. *Macromolecules* **1985**, *18*, 1753.
(2) Onsager, L. *Ann. N. Y. Acad. Sci.* **1949**, *51*, 627.
(3) Flory, P. J. *Proc. R. Soc. (London), Ser. A* **1956**, *234*, 73.

(4) Flory, P. J. *Macromolecules* **1978**, *11*, 1141.
(5) Maier, W.; Saupe, A. *Z. Naturforsch.* **1959**, *149*, 882; *Z. Naturforsch.* **1960**, *159*, 187.
(6) Dalmolen, L. G. P.; Picken, S. J.; De Jong, A. F.; De Jeu, W. H. *J. Phys.* **1985**, *46*, 1443.
(7) Ying, Q.; Chu, B. *Makromol. Chem., Rapid Commun.* **1984**, *5*, 785.
(8) Cotter, M. A. *Mol. Cryst. Liq. Cryst.* **1977**, *39*, 173.
(9) Luckhurst, G. R. In *Molecular Physics of Liquid Crystals*; Luckhurst, G. R.; Gray, G. W., Eds.; Academic: London, 1979; pp 85–119.
(10) Jähnig, F. *J. Chem. Phys.* **1979**, *70*(7), 3279.
(11) Warner, M.; Gunn, J. M. F.; Baumgartner, A. *J. Phys.* **1985**, *18*(A), 3007.
(12) Cifferi, A.; Marsano, E. *Gazz. Chim. Ital.* **1987**, *117*, 567.
(13) Lenz, R. W. *Farady Disc. Roy. Soc.* **1985**, *79*, 21.
(14) Roviello, A.; Sirigu, A. *Gazz. Chim. Ital.* **1979**, *107*, 333.
(15) Sikkema, D. J.; Hoogland, P. *Polymer* **1986**, *27*, 1443.
(16) ten Bosch, A.; Maissa, P.; Sixou, P. *Phys. Lett.* **1983**, *94*(A) 298; *J. Chem. Phys.* **1983**, *79*, 3462; *J. Phys. Lett.* **1983**, *44*, L105.
(17) Khokhlov, A. R.; Semenov, A. N. *Stat. Phys.* **1985**, *38*(1/2), 161.

Poly[(ω-carboxy)oligo(oxyethylene) methacrylate] as a New Type of Polymeric Solid Electrolyte for Alkali-Metal Ion Transport

Eishun Tsuchida,* Hiroyuki Ohno, Norihisa Kobayashi, and Hajime Ishizaka

Department of Polymer Chemistry, Waseda University, Tokyo 160, Japan.
Received January 14, 1988; Revised Manuscript Received September 26, 1988

ABSTRACT: Alkali-metal salts of (ω-carboxy)oligo(oxyethylene) methacrylate (CME$_n$M, M = Li, Na, or K) have been synthesized and polymerized to prepare polymeric solid electrolytes. These polymers have a flexible main chain, an oligo(oxyethylene) side chain for ion conduction, and a carrier ion source in the repeating unit. The conductivity of CME$_7$K homopolymer, 1.1×10^{-7} S/cm at 30 °C, is the highest value reported for a polyelectrolyte "homopolymer" without any additives. This conductivity is attributed to the oligo(oxyethylene) side chain, which facilitates the dissociation of the alkali-metal carboxylate. The temperature dependence of ionic conductivity is not linear, suggesting that conduction occurs by the WLF mechanism. Vogel–Tammann–Fulcher plots are linear when the standard temperature is defined as $T_g - 50$ °C. The differences in conductivity of P(CME$_7$M) with different cations at the same ΔT from T_g are attributed to differences in ion–dipole interaction forces and in dissociation energy of the electrolyte. WLF plots of the conductivity of P(CME$_n$M) are independent of cation species and show a standard curved line, suggesting that carrier ions do not migrate naked but are bound to polymer segments through ion–dipole interaction forces. It is suggested that ion migration is controlled primarily by segmental motion of the polymer rather than by the interaction between cation and ether oxygen.

Introduction

Polymeric solid electrolytes with high ionic conductivity are of interest for theoretical and basic research as well as for applications in novel devices. Research on polyether/inorganic salt hybrids has been aimed at achieving higher conductivity and analyzing the ionic conduction mechanism.[1-9] These polymeric solid electrolytes containing LiClO$_4$ have ionic conductivities of 10^{-6}–10^{-9} S/cm at 25 °C. We have reported an ionic conductivity as high as 10^{-5} S/cm in poly[oligo(oxyethylene) methacrylate]/LiX.[10-12] This ionic conductivity was attributed to the flexible oligo(oxyethylene) segment with a lower T_g than crystalline poly(oxyethylene). Comblike polymers containing oligo(oxyethylene) chains have been used as matrix polymers, and their hybrids with inorganic salts showed similar conductivities.[13-16]

These hybrid polymeric solid electrolytes do not prevent the migration of counterions. Accordingly, a significant decrease in ionic conductivity occurs under continued dc polarization even when alkali-metal nonblocking electrodes are used. It appears that ion pairs are localized near the anode. This localization could increase the T_g of the microenvironment in the polymeric solid electrolyte, thus blocking ion migration and preventing further supply of alkali-metal cations from the anode. This decrease in conductivity bars the use of such electrolytes in devices driven under dc polarization and points to the need for a matrix in which only cation migration is allowed.

There are three approaches to single-ion conduction in a polymer matrix. (1) Blends of polyelectrolyte salts with soft segments such as poly(oxyethylene), in which countercations become mobile,[17,18] are one approach. This selective ion conduction can be attributed to the relatively larger diffusion coefficient of small counterions than that of the giant polyions. (2) Polyelectrolyte "copolymer" systems that contain units with relatively large segmental motion are another. We have reported on copolymers of oligo(oxyethylene) methacrylate and alkali-metal methacrylates as polymeric solid electrolytes that have a carrier ion source and a low T_g matrix and that show high ionic conduction without any additives.[19-21] (3) Polyelectrolyte "homopolymers" are a third approach. We report here the synthesis of alkali-metal salts of (ω-carboxy)oligo(oxyethylene) methacrylate and the preparation of polymeric solid electrolytes from them by polymerization.

Experimental Section

Materials. (ω-Carboxy)oligo(oxyethylene) Methacrylate (CME$_n$H). (ω-Hydroxy)oligo(oxyethylene) methacrylate (Blenmer, Nippon Oil & Fats Co., Ltd.) (20 g for n = 3, 30 g for n = 7) and NaHCO$_3$ (8 g) were dissolved in 500 mL of distilled water. This solution was vigorously stirred with 6 g of 10% platinum-on-carbon catalyst while oxygen was bubbled through. The reaction temperature was maintained under 40 °C to avoid spontaneous polymerization. After 12 h, the catalyst was filtered out and washed well with distilled water to collect monomers. The resulting aqueous solution was adjusted to pH 2 with hydrochloric acid to remove carbonate ion, and the pH was then increased to 8 with aqueous lithium hydroxide solution. The solution was washed with chloroform (500 mL × 6) to remove the unreacted Blenmer. The pH of the solution was again changed to 2, and CME$_n$H was extracted with chloroform. The extract was diluted

0024-9297/89/2222-1771$01.50/0